

Irina SEMENOVA,\* Petr HORYL\*\*

THE INFLUENCE OF THE BASIC PARAMETERS OF THE NUMERICAL MODEL ON THE  
CONTACT PRESSURE IN DYNAMIC TASKS

VLIV ZÁKLADNÍCH PARAMETRŮ NUMERICKÉHO MODELU NA KONTAKTNÍ TLAKY V  
DYNAMICKÝCH ÚLOHÁCH

**Abstract**

The paper is devoted to quasi-static and low-velocity impact simulation using finite element modelling. The paper describes the effects of contact models, contact parameters, integration method, and the velocity of impact on contact stresses values. Pure Penalty, Lagrange Multiplier, and Augmented Lagrange Multiplier with various friction factors were used as contact algorithms. The influence of Newmark's integration method and the central difference time integration method on the resultant stresses is discussed.

**Abstrakt**

Příspěvek je věnován simulaci kvazistatického a nízko rychlostního rázu metodou konečných prvků. Článek popisuje účinky kontaktních modelů, kontaktních parametrů, metod integrace a rychlosti dopadu na hodnoty kontaktního namáhání. Jako kontaktní algoritmy byly použity přístupy Pure Penalty, Lagrange Multiplier a Augmented Lagrange Multiplier s různými hodnotami součinitele tření. Byl sledován vliv Newmarkovy integrační metody a metody centrálních diferencí na vyhodnocovaná napětí.

## 1 INTRODUCTION

The finite element method (FEM) is a widespread numerical method nowadays. It is widely used for modelling contacts between parts of systems. The importance of simulating diverse kinds of contacts for static or transient types of analysis has led to the constant development or modification of contact models. The main common widespread algorithms that are frequently used in commercial FEM software are Pure Penalty (PP), Lagrange Multiplier (LM), and Augmented Lagrange Multiplier (ALM) [1,2]. The problem is how to choose appropriate algorithm parameters depending on the type of analysis.

Moreover, simulation systems with contact are extremely “expensive” with regard to computer time costs. That is why in some tasks in which the use of small time steps is necessary, we may prefer an explicit solution method instead of an implicit time integration method. In those cases it is important to know the influence of the integration method on contact result stresses.

So the main aim of the work is an examination of the effects of contact model parameters and the solution method on contact stresses achieved by quasi-static and low-velocity impact simulation.

---

\* Ing., VŠB – Technical University of Ostrava, Faculty of Mechanical Engineering, Department of Mechanics, 17. listopadu 15, Ostrava – Poruba, tel. (+420) 59 732 5283, e-mail: irina.semenova.st@vsb.cz

\*\* prof. Ing. CSc. dr.h.c., VŠB – Technical University of Ostrava, Faculty of Mechanical Engineering, Department of Mechanics, 17. listopadu 15, Ostrava – Poruba, tel. (+420) 59 732 4351, e-mail: petr.horyl@vsb.cz

## 2 NUMERICAL MODEL

A constrained wedge and a ring with a thickness of 10 mm are used as a target and a contact body respectively. The ring with a velocity  $V_0$  strikes the wedge surface at an angle  $\alpha$ . After the contact it rebounds at an angle  $\beta$  with a velocity  $V_1$ . The dimensions of the model are shown in Figure 1. The material properties are as follows: for steel, the elastic modulus  $E = 2 \cdot 10^{11}$  MPa, the Poisson coefficient = 0.3, and the density  $\rho = 7850 \text{ kg/m}^3$ ; for bronze, the corresponding values are  $1 \cdot 10^{11}$  MPa, 0.34, and  $8300 \text{ kg/m}^3$ .

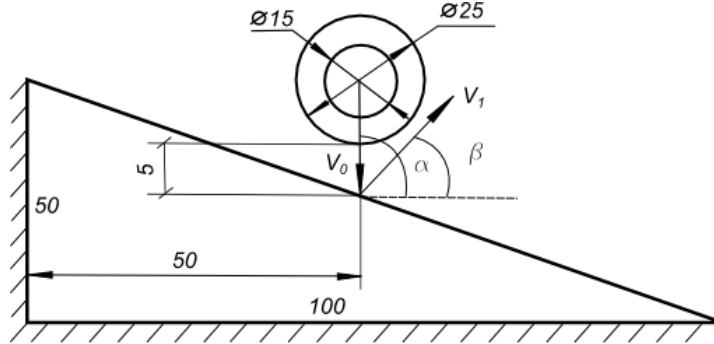


**Fig. 1** Model parameters

The contact problem was solved by FEM in ANSYS 14.0. The basis of the method is solving the matrix differential equation of motion via Newmark's integration method (implicit) or the central difference time integration method (explicit). For the model of motion the equation would be:

$$[M]\{\ddot{u}\} + [C]\{\dot{u}\} + [K]\{u\} + [K_k]\{u\} = 0,$$

where  $[M]$  is the mass matrix,  $[C]$  is the damping matrix,  $[K]$  is the stiffness matrix,  $\{u\}$  is the displacement vector, and  $[K_k]\{u\}$  is the nonlinear contact force. The initial conditions were  $\{u\}_0 = 0$  for the initial displacement, and  $\{\dot{u}\}_0^{ring} = -30, -3 \text{ m/s}$ .

The node displacements of a discrete model are the results of the solution. Geometric discretization was done by using the isoparametric SOLID 185 (implicit) and SOLID 164 (explicit) as finite elements. Every element has eight nodes with three degrees of freedom (DOFs) in each node and linear shape function.

The presence of nonlinear contact forces causes a nonlinear part to appear in the motion equation. This part was numerically computed by three algorithms: PP, LM, and ALM. The solution is found when a minimum of potential energy is achieved. The equations of potential energies for the contact models are presented in Table 1. Friction was modelled by a simple Coulomb friction model with a static versus dynamic factor ratio of  $\mu_s/\mu = 1$ .

**Tab. 1** Potential energy in the contact algorithms

	Principle	Potential energy	Description
Pure Penalty	Contact spring stiffness	$\Pi(u) = \Pi_0 + \frac{1}{2}[G]^T[k][G]$	[G] – displacement matrix, [k] – stiffness matrix of additional contact springs,
Lagrange Multiplier	Contact forces as Lagrange multipliers	$\Pi(u, \Lambda) = \Pi_0 + [\Lambda]^T[G]$	
Augmented Lagrange Multiplier	Combination of Pure Penalty and Lagrange Multiplier	$\Pi(u, \Lambda) = \Pi_0 + \frac{1}{2}[G]^T[k][G] + [\Lambda]^T[G]$	[Λ] – matrix of Lagrange multipliers

Geometric finite element discretization was chosen after the convergence testing. The influence of the mesh size on the solution was investigated. The model is considered to be convergent when the solution parameters approach a fixed value. An equivalent von Mises stress was chosen as the solution parameter, because of the presence of the triaxial stress state in the contact area. The equivalent von Mises stress is computed as:

$$\sigma_e = \left[ \frac{(\sigma_1 - \sigma_2)^2 + (\sigma_2 - \sigma_3)^2 + (\sigma_3 - \sigma_1)^2}{2} \right]^{1/2},$$

where  $\sigma_1, \sigma_2,$  and  $\sigma_3$  are the principle stresses.

For convergence testing, four models with different sizes of the elements ( $\Delta = 0.4, 0.5, 1.0,$  and  $2.0$  mm) in the contact area were developed. They consisted of 165601 to 70289 nodes with 1324808 to 562312 DOFs. The examples of finite element models with minimum and maximum element size are shown in Figure 2. Contact was modelled by the Pure Penalty algorithm with a penalty scale factor  $NPS = 1$  and without friction  $\mu_D = 0$ .

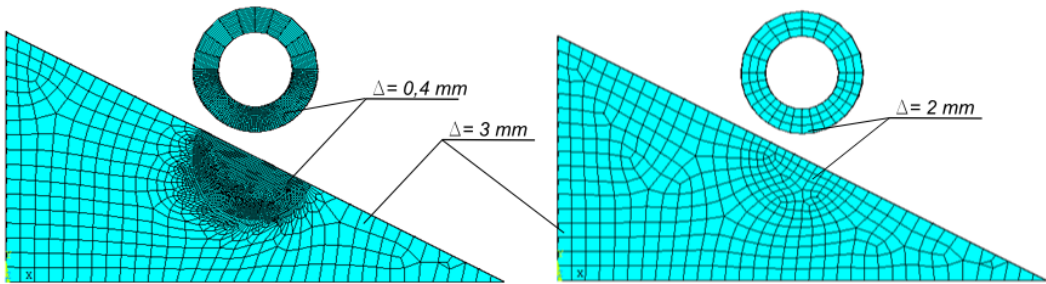


**Fig. 2** Finite element models

In Figure 3 the maximum values of the equivalent von Mises stress in the contact area versus  $1/\Delta$  are given. According to the graph, the contact elements of  $0.5$  mm size ( $1/\Delta = 2 \text{ mm}^{-1}$ ) were finally selected for the analysis.

Time discretization for the implicit transient analysis was established by using a uniform time step size of  $0.1 \mu\text{s}$ . The whole solution time was set to  $3 \mu\text{s}$ . Contact lasted from  $1.2$  to  $1.3 \mu\text{s}$ . For an explicit transient analysis the time step size was chosen automatically according to the Courant criterion:  $\Delta t = l/c$ , where  $l$  is the minimum element size, and  $c = \sqrt{E/\rho}$  is the wave velocity in material. Thus the time step size varied from  $0.08$  to  $0.4 \mu\text{s}$ . To compare the results computed by two different integration methods, the output time step for the explicit analysis was set to  $0.1 \mu\text{s}$ .

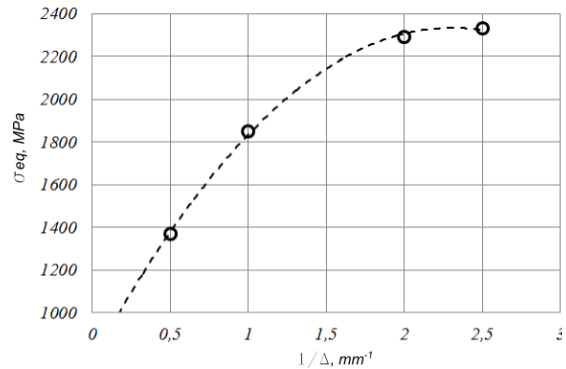


**Fig. 3** Relation between equivalent von Mises and stress element size

### 3 RESULTS

The effect of the chosen contact model and the integration algorithm as well as the ring velocity on the equivalent von Mises stress and normal/tangential contact pressures was studied. The investigation was done by using different penalty scale factors ( $NPS = 1, 5, 10, 20$ ) and dynamic friction factors ( $\mu = 0, 0.1, 0.2, 0.3, 0.5$ ) and two initial velocities of the ring,  $V = 3$  and  $30$  m/s. The influence of the contact methods and the ring velocity of  $30$  m/s on the maximum equivalent von Mises stress in the contact area is presented in Table 2 and Figure 4.

**Tab. 2** Equivalent von Mises stress (ring velocity of  $30$  m/s)

$N$	$\mu$	$PP,$ $NPS = 1$	$PP,$ $NPS = 10$	$LM$	$ALM$	$Explicit,$ $PP^*$ $NPS = 1$	$Explicit,$ $PP$ $NPS = 10$
		$max\sigma_{eq}, Mpa$					
1	0	1880	1930	2520	2520	1358	1909
2	0.1	1990	2130	2540	2560	1455	1833
3	0.2	2240	2390	2490	2520	1519	1922
4	0.5	2990	3000	3200	3190	1852	2214

\* “Explicit, PP” means the Pure Penalty contact algorithm with the explicit integration method

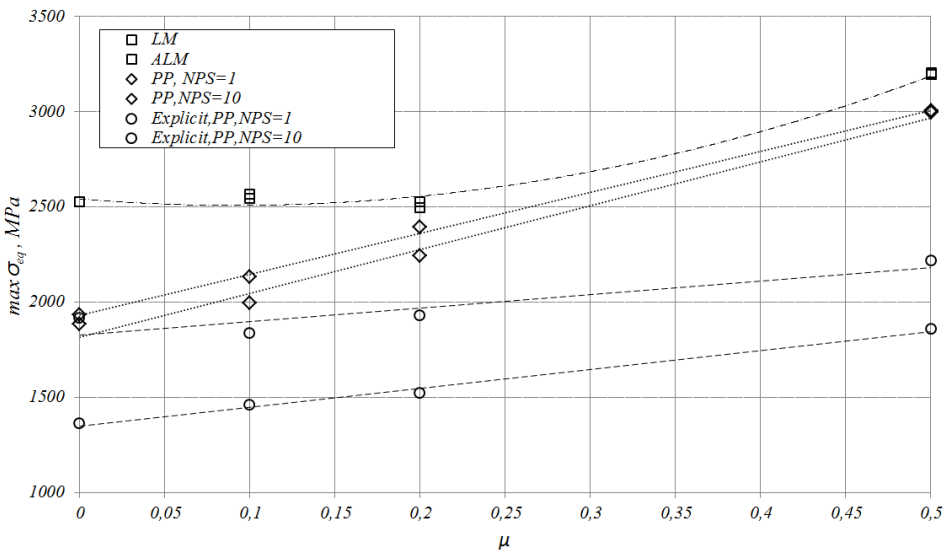


**Fig. 4** Equivalent von Mises stress versus friction factor for the contact algorithms (ring velocity:  $30$  m/s)

The contact and integration algorithms generate a significant effect on the equivalent von Mises stresses produced by low-velocity impact ( $V = 30$  m/s). The maximum difference between PP and LM results with the implicit integration method achieves a value of 25%. Comparing the explicit and implicit integration methods while using the same PP contact algorithms, a difference of about 40% ( $FKN = 1, \mu = 0$ ) was found. By the way, LM and ALM produce the same equivalent stresses. With increases in the dynamic friction coefficient value, the equivalent stresses tend to rise. Obviously this depends on increases in the tangential stresses due to the presence of friction.

Analysis of normal contact pressures reveals that normal stresses under low-velocity impact change as the friction coefficient increases (Fig. 5a, Tab. 3). The PP algorithm gives a decrease in the

normal pressures of about 10%, but Lagrange-based algorithms give an increase of about the same value. Using the explicit integration method with a default value of  $FKN = 1$  produces minimal values of the normal contact pressures that are significantly different (about 30% lower) from the others.

Tangential contact pressures are shown in Fig. 5b. The results of all of the contact models show a difference of about 16% only when the friction coefficient  $\mu = 0.5$ . In other ways the tangential pressures show a good correlation with each other.

**Tab. 3** Normal and tangential contact pressures, MPa (ring velocity: 30 m/s)

$N$	$\mu$	$PP,$ $NPS = 1$	$PP,$ $NPS = 10$	$LM$	$ALM$	$Exp.,PP,$ $NPS = 1$	$Exp.,PP,$ $NPS = 10$	$Exp.,PP,$ $NPS = 20$
		<i>Norm/Tan</i>				<i>Norm</i>		
1	0	2990/0	3310/0	2860/0	2860/0	2103	2769	2887
2	0.1	2990/299	3260/326	2910/291	2920/292	2093	2750	2914
3	0.2	2960/592	3190/637	3030/606	3030/606	2045	2737	2869
4	0.5	2900/1320	3010/1430	3260/1570	3260/1570	1887	2653	2703

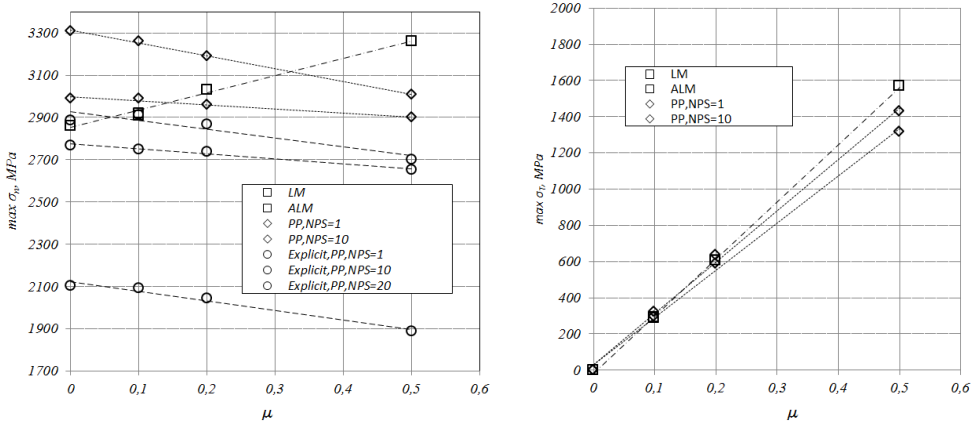


**Fig. 5** Normal (left) and tangential (right) contact pressures (ring velocity: 30 m/s)

The dependence of normal pressures on the contact algorithms at quasi-static contact interactions ( $V = 3\text{m/s}$ ) almost disappears (Fig. 6, Tab. 4). With the implicit integration method, the difference between the PP and LM algorithms is about 1.5%. The explicit integration method with a default value of  $FKN = 1$  produces the maximal difference (5%) from the results given by implicit PP.

**Tab. 4** Normal contact pressures, MPa (ring velocity: 3 m/s)

$N$	$\mu$	$PP,$ $NPS = 1$	$LM$	$ALM$	$Exp.,PP,$ $NPS = 1$	$Exp.,PP,$ $NPS = 5$	$Exp.,PP,$ $NPS = 10$
1	0	567	575	575	407	544	544
2	0.2	571	576	576	401	536	655
3	0.3	572	576	576	401	541	542

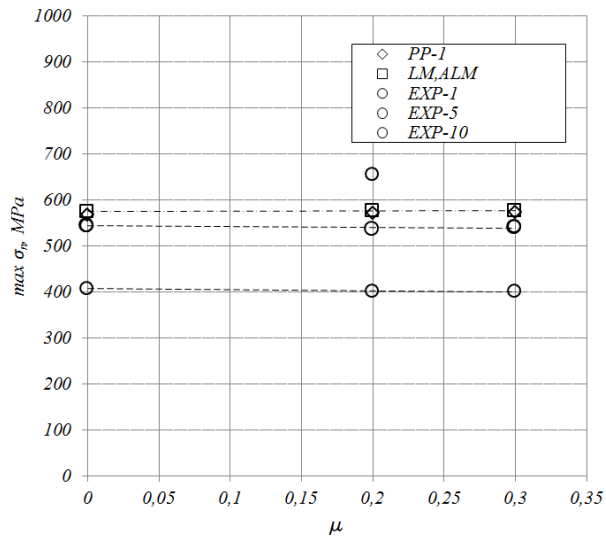


**Fig. 6** Normal contact pressures (ring velocity: 3 m/s)

## 6 CONCLUSIONS

The effect of the three contact numerical algorithms and the two integration algorithms as well as the impact velocity on the equivalent von Mises stress and normal/tangent contact pressures was investigated by using the commercial numerical code ANSYS 14. Seventy different variants were analysed. The analysis reveals that:

1. At a low-velocity impact, the contact stresses depend on contact models and their parameters, integration methods, and a friction coefficient.
2. The explicit method with a default penalty scale factor of 1 produces minimal values of contact stresses, differing from the equivalent Pure Penalty model solved by the implicit method by about 40% (low-velocity impact) and 5% (quasi-static impact).
3. Under a quasi-static impact there is no dependence on contact models and friction coefficients, but Lagrange-based algorithms produce relatively higher values (by about 1.5%) of the contact pressures.

## ACKNOWLEDGEMENTS

The paper has been done in connection with project IT4Innovations Centre of Excellence project, reg. no. CZ.1.05/1.1.00/02.0070 supported by Operational Programme "Research and Development for Innovations" funded by Structural Funds of the European Union and state budget of the Czech Republic.

## REFERENCES

- [1] WRIGGERS, P. *Computational contact mechanics*. 2nd ed. Heidelberg: Springer, 2006.
- [2] SEXTRO, W. *Dynamical contact problems with friction. Models, methods, experiments and applications*. Springer, 2nd ed. 2007, 190 p., ISBN-10: 3540695354.